Comparing Viral (HIV) and Bacterial (*Staphylococcus aureus*) Infection of the Bone Tissue

Mohammad Ali Moni[1], Pietro Liò[1] and Luciano Milanesi[2]
[1]*Computer Laboratory, Cambridge University, William Gates Building, 15 JJ Thomson Avenue, Cambridge CB3 0FD, U.K.*
[2]*Institute for Biomedical Technologies, Via Fratelli Cervi, 93 20090, Segrate, Italy*

Keywords: Osteomyelitis, HIV, Staphylococcus aureus.

Abstract: This paper focuses on the differences between *S. aureus* bacterial and HIV viral infection of the bone tissue. Both of these infections alters the RANK/RANKL/OPG signalling dynamics that regulates osteoblasts and osteoclasts behavior in bone remodelling. These infections rapidly lead to severe bone loss and it may even spread to other parts of the body. Since both HIV and osteomyelitis cause loss of bone mass, we focused on comparing the dynamics of these diseases by means of computational models. Firstly, we performed meta-analysis on the gene expression data of normal, HIV and osteomyelitis bone conditions and compare the effects of HIV and *S. aureus* infection. We mainly focused on RANKL/OPG signalling, the TNF and TNF receptor superfamilies and the NF-kB pathway. Using information from the gene expression data, we estimated parameters for a novel model of osteomyelitis. Then we develop another multi strain HIV ODE model incorporating the HAART therapy. Our ODE modelling aims at investigating the dynamics of the effects of osteomyelitis and HIV infection in bone remodelling.

1 INTRODUCTION

Bone remodelling is a cellular process conducted by *osteoclasts*, the cells responsible for bone resorption and by *osteoblasts*, the cells responsible for bone formation. Another type of cells, the *osteocytes*, are trapped in the bone matrix and these cells play a relevant role in the remodelling process. In normal bone, the bone resorption and bone formation rate are all relatively constant (Raggatt and Partridge, 2010). But pathological conditions such as cancer, infection and autoimmune diseases can alter the equilibrium between bone resorption and bone formation, reducing bone density and increasing the risk of spontaneous fractures.

The *RANK/RANKL/OPG* signalling pathway plays an important role in bone metabolism. RANK is a protein expressed by osteoclasts and it is a receptor for RANKL, a protein produced by osteoblasts. RANK/RANKL signalling triggers osteoclast differentiation, proliferation and activation, thus it prominently affects the resorption phase during bone remodelling. Osteoprotegerin (OPG) is a decoy receptor for RANKL. It is expressed by mature osteoblasts and it binds to RANKL, thus inhibiting the production of osteoclasts. While under normal circumstances, the ratio of RANKL/OPG is carefully balanced and the increase of RANKL plays an essential role in favouring resorption through osteoclast formation, function, and survival.

Osteomyelitis is characterized by severe and rapid bone loss. It is a bone infection mainly caused by the aggressive pathogen *S. aureus*. The action of *S. aureus* increases RANKL expression and decreases OPG expression in osteoblasts in patients with staphylococcal osteomyelitis. The increase in RANKL is likely to trigger osteoclast-induced bone resorption and bone destruction that may help to explain patients with osteomyelitis have significant bone loss (Claro et al., 2011).

On the other hand, infection with the human immunodeficiency virus-1 (HIV) and the resulting acquired immune efficiency syndrome (AIDS) affect not only cellular immune regulation but also the bone metabolism (Reem et al., 2011). It is observed that significant number of HIV-1 infected patients exhibit osteopenia and osteoporosis, leading to higher incidence to develop weak and fragile bones during the course of disease (Gibellini et al., 2008). Patients with HIV infection have decreased numbers of osteoblasts, decreased bone mineralization and increased risk of fracture compared to age and sex matched HIV unin-

Ali Moni M., Liò P. and Milanesi L..
Comparing Viral (HIV) and Bacterial (Staphylococcus aureus) Infection of the Bone Tissue.
DOI: 10.5220/0004249801960201
In *Proceedings of the International Conference on Bioinformatics Models, Methods and Algorithms* (BIOINFORMATICS-2013), pages 196-201
ISBN: 978-989-8565-35-8

fected patients. However, the molecular mechanisms behind these associations remain unclear (Cummins et al., 2011).

So considering the both *S. aureus* and HIV infection, we develop a hybride modelling framework for combining and untangling the relationships of physiological and molecular data. We then apply the methodology to determine disease related abnormalities of the key osteogenesis molecular network. We believe that this framework could easily be adapted to model also other bone diseases like multiple myelomas or Paget's disease, and that could help in better understanding the disruptions of cellular and signalling mechanisms that underlie such bone pathologies.

2 METHODS

2.1 Data Analysis and ODE Models

For our meta analysis, we have considered 5 different human microarray data sets from the Gene Expression Omnibus ($http://www.ncbi.nlm.nih.gov/geo/$), accession numbers are GSE16129, GSE6269, GSE11907, GSE11908, and GSE18464 (Ardura et al., 2009; Ramilo et al., 2007). We observe that RANKL, RANK, OPG and NF-kB proteins impact more on the bone remodelling for osteomyelitis and osteoporosis (Ramilo et al., 2007; Ardura et al., 2009). For this reason to understand the effect of *S. aureus* and HIV on osteomyelitison bone remodelling, we have taken in account all the genes TNF and TNF receptor superfamilies including the genes related to the proteins RANKL, RANK, OPG and NF-kB proteins. We have selected samples of 48 infected and 27 healthy controls for *S. aureus*. In case of HIV infection, we choose 22 data samples of low viral loads (LVL, $<=$ 10,000 RNA copies/ml), 22 data samples of high viral loads (HVL, $=>$ 10,000 RNA/copies/ml) and 11 healthy controls. The data sets contain data from people of different age and sex. Here, normalization procedures and statistical analysis are performed by using Bioconductor R packages (Gentleman et al., 2004). Standard anova and Box plots representation were used to analyze and visualize the expression levels of these genes for the *S. aureus* and HIV infection conditions. For presenting the signaling and interaction pathways of the genes, we used cytoscape for data integration and network visualization (Smoot et al., 2011) and reactome functional interaction (FI) cytoscape plugin for knowledge base of human biological pathways and network processes (Joshi-Tope et al., 2005).

We have implemented the ODE models in *C++*, *R*, and using the bioconductor package *FME* package (Soetaert et al., 2010) to analyse parameter sensitivity and robustness. We have used *MATLAB* for steady states and ODE calculation using state of art numerical routines. In our models, most of the parameters are from biological literature and from the gene expression data. Even parameters from the mathematical modelling literatures are estimated from biological experimental studies.

3 RESULTS AND DISCUSSION

3.1 Bioinformatics of *S. aureus* and HIV

Since that both *S. aureus* and HIV cause loss of bone mass, we decided to cross-compare the gene expression data sets of both pathogens infection. We have compared the expression levels of genes involved in *S. aureus* causes osteomyelitis, HIV infection and healthy controls using the box plots and polar histogram (see Figure 1 and 2).

From the analysis of our gene expression data (GSE16129, GSE6269, GSE11907, GSE11908), we observe that few genes, related to TNF, TNF receptor superfamilies including RANKL, RANK, OPG and NF-kB have statistically different levels of expression in osteomyelitis and or HIV infection compare to the healthy controls. We observe that, with respect to control cases, TNFSF10, TNFSF12, TNFSF13, TNFRSF10B, TNFRSF10C, TNFRSF1A, TNFRSF1B, NFKB2, REL and RELB genes related to RANKL, RANK, OPG, NF-kB proteins, TNF and TNF receptor superfamilies are over expressed and TNFRSF14, TNFRSF25, TNFSF11, NF-kB1 and RELA genes are down regulated in *S. aureus* caused osteomyelitis (see Figure. 1).

From the meta analysis of the HIV infection, we observe that TNF, TNFSF4, TNFSF13, TNFRSF8, TNFRSF10A, TNFRSF21, TNFAIP3 and TNFAIP6 genes are up regulated and TNFSF13B, TNFSF18, TNFSF11, TNFRSF10C, TNFRSF10D, TNFAIP8 and TNFAIP8L2 are down regulated (see Figure. 2). It is notable only TNFSF13 is up-regulated in both types of diseases and TNFSF11 (RANKL genes) is down regulated in the both osteomyelitis and HIV infection.

Interestingly we found that, despite of increasing RANKL gene expression in osteomyelitis, OPG gene expression become more deregulated in osteomyelitis. Therefore we report that gene expression in HIV and osteomyelitis could generate an unbalance between RANKL and OPG, but also other genes, re-

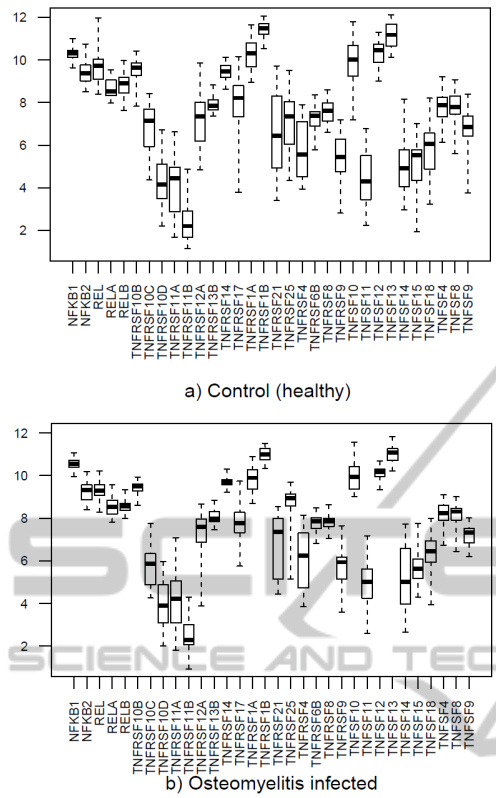

Figure 1: Expression level (y axis) of the 32 genes (x axis) of the human osteoclasts corresponding to a) 27 healthy controls and b) 48 *S. aureus* caused osteomyelitis infected patients.

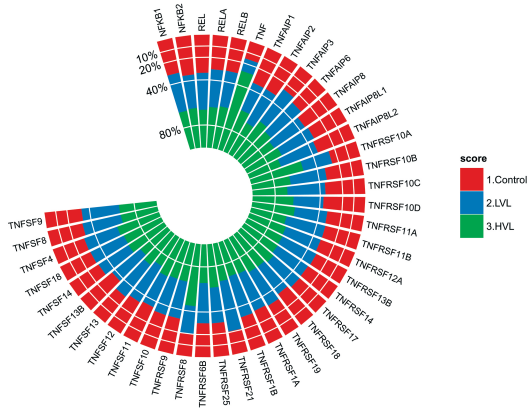

Figure 2: Average expression level of the genes are compared among healthy control, low viral level and high viral level infected patients.

lated to TNF, TNF receptor superfamilies and to NF-kB may be involved. Finally, we showed signaling pathways of these genes and grouped based on their interaction pathways (see Figure. 3).

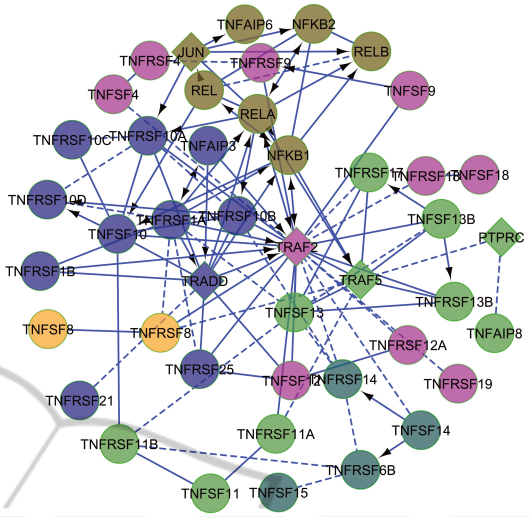

Figure 3: Network of the 44 genes related to the NF-kB, tnf and tnf receptor super families including RANKL, RANK and OPG. The network includes both up and down regulated genes, on the basis that both will potentially appear in a single differentially expressed pathway. Circular nodes are genes in the microarray data sets, while diamond shaped nodes are linkers, that were determined programmatically to connect the circular nodes in a network. The whole network is clustered based on the signaling pathways and showed each pathway using individual color.

3.2 Cell Interaction Models

Although gene expression and actual protein abundance are only loosely correlated, taking into account the results of gene expression data, we modified the autocrine and paracrine parameters of the existing mathematical model based on Komarova model (Komarova et al., 2003). We considered more appropriate to incorporate into the model the algebraic relationship of positive and negative regulators (such as RANKL and OPG) than just the RANKL change. On the basis of this consideration we developed new models for reproducing osteomyelitis conditions. Then we developed a multistrain HIV model including the RANKL and OPG gene expression level with condition.

3.2.1 Bacterial Infection Model

We develop a differential equation model for describing the dynamics of bone remodelling and of bone-related pathologies at a multicellular level. The model describes the continuous changes and the interactions between populations of osteoclasts and osteoblast. Our cellular-level model is based on the work by Komarova et al (Komarova et al., 2003), where they developed an important model for bone remodelling

based on experimental results described in Parfitt's work (Parfitt, 1994) which has inspired many other similar models.

The ODE model for bone remodelling describes the dynamics of osteoblasts' (Ob) and osteoclasts' (Oc) population and calculates the bone density as a function of Ob and Oc. The model describes the autocrine and paracrine relationships between osteoclasts (Oc) and osteoblasts (Ob).

Here the parameters g_{ij} describe the effectiveness of autocrine and paracrine regulation, g_{11} describes the osteoclast autocrine regulation, g_{22} is the osteoblast autocrine regulation, g_{21} is the osteoblast-derived paracrine regulation, and g_{12} is the osteoclast paracrine regulation. The autocrine signalling has a positive feedback on osteoclast production ($g_{11} > 0$), and paracrine signalling has a negative feedback on osteoclast production ($g_{21} < 0$). The autocrine signaling has a positive feedback on osteoblast production ($g_{22} > 0$), and paracrine signalling has a positive feedback on osteoblast production ($g_{12} > 0$). The overall regulatory circuit should lead to a positive mineralisation balance (z) which could be described by the expression $\frac{dz}{dt} = -k_1 O_c + k_2 O_b$ where k_1 and k_2 are the resorption and formation rates, respectively. The bone density is determined by the difference between the actual resorption and formation activity when osteoclasts and osteoblasts exceed their steady levels. Therefore bone density is calculated as a function of z. Moreover, we introduced the regulation factors in order to model an increased RANKL expression by osteoblasts, which results both from the analysis performed on gene expression data and from experimental evidences (Morabito, 2004). In our model g_{21} is the result of all the factors produced by osteoblasts that activates osteoclasts and as explained in (Komarova et al., 2003), $g_{21} = RANKL - OPG$ where $RANKL$ is the effectiveness of RANKL signalling while OPG is the effectiveness of OPG signalling.

Starting from this, we consider the progressing of osteomyelitis induced by the *S. aureus* (variable B). Since several evidences show that the dynamics of the bacterial population follows a Gompertz curve, we consider an equation of the form $\frac{dB}{dt} = \gamma_B B \cdot log(\frac{s}{B})$, where γ_B is the growth rate of bacteria, and s is the carrying capacity, i.e. the maximum population size. Additionally, we introduced four parameters f_{ij} used to model the effects of the infection on the autocrine and paracrine regulation factors g_{ij}. The resulting equations are:

$$\frac{dO_c}{dt} = \alpha_1 O_c^{g_{11}(1+f_{11}\frac{B}{s})} O_b^{g_{21}(1-f_{21}\frac{B}{s})} - \beta_1 O_c, \quad (1)$$

$$\frac{dO_b}{dt} = \alpha_2 O_c^{g_{12}/(1+f_{12}\frac{B}{s})} O_b^{g_{22}-f_{22}\frac{B}{s}} - \beta_2 O_b, \quad (2)$$

$$\frac{dz}{dt} = -k_1 max(O_c - \bar{O}_c, 0) + k_2 max(O_b - \bar{O}_b, 0) \quad (3)$$

$$\frac{dB}{dt} = (\gamma_B - V) B \cdot log(\frac{s}{B}). \quad (4)$$

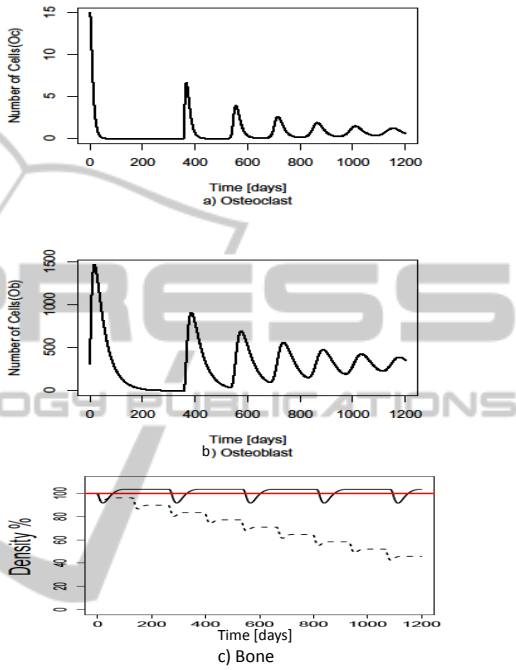

Figure 4: Simulation results of the ODE model. The osteomyelitis condition affects the osteoclast, osteoblast patterns and bone density. In x axis time in days and y axis the local cell density. In case of bone density figure, red line represents the steady state, black line represents the healthy condition and dashed line is the effect of osteomyelitis.

Here, we introduced four parameters: f_{ij} used to model the effects of the infection on the autocrine and paracrine regulation factors g_{ij}. The bacterial parameters f_{11}, f_{12}, f_{21}, f_{22} are all nonnegative. $\bar{O}_c$ and $\bar{O}_b$ denote the steady states of O_c and O_b, respectively. The *S. aureus*-induced infection affects the normal remodelling activity by reducing osteoblasts' growth rate and increasing RANKL and decreasing OPG expression. The parameter V describes the effectiveness of the antibiotic treatment as a factor decreasing the growth rate γ_B of bacteria. Two different kinds of treatment can be distinguished: bacteriostatic treatments that stop bacteria proliferation ($V = \gamma_B$); and bacteriocide treatments which kill bacteria ($V > \gamma_B$). Simulation results for osteoclasts, osteoblasts and bone density are compared in Figure 4.

3.2.2 HIV Infection Model

Here, our work is based on the evolution of a multi-strain ode model of HIV-1 dynamics, firstly appeared in (Sguanci et al., 2007). These models are well presented and take specific biological reality into account and the effect of the RANKL, which is the main issue for osteomyelitis and bone remodelling. Furthermore, we have introduced an abstract representation of the HAART therapy treatment by including the necessary parameters that rule the dynamics of our model according to the known effects of the treatment. Mutation parameter μ generates additional strains of virus from existing phenotype strains. Here, we have considered k different strains of viral particles and infected cells.

The interactions among the immature T cells (U), uninfected mature T cells (T), infected cells (I), viral strains (V) and RANKL signaling (G) are translated into following system of ordinary differential equations (ODEs):

$$\frac{dU}{dt} = \lambda - \delta_{ut}U - \delta_u U \sum_k V_k - \delta_{ug} U G \quad (5)$$

$$\frac{dT_i}{dt} = \delta_{ut}U - \sum_k (1-\eta_{RT})\beta_k V_k T_i - \delta_t T_i - \alpha_{ti} T_i I_k \quad (6)$$

$$\frac{dI_k}{dt} = \left(\sum_{k'} \mu_{kk'}(1-\eta_{RT})\beta_{k'} V_{k'}\right)\left(\sum_i T_i\right) - \delta_i I_k + \alpha_{ti} T_i I_k \quad (7)$$

$$\frac{dV_k}{dt} = (1-\eta_{PI})\pi I_k - \delta_v V_k \quad (8)$$

$$\frac{dG}{dt} = \sigma \sum_k V_k \quad (9)$$

Equation (5) describes the constant production of immature T cells by the thymus at rate λ and their transformation into mature T cells at rate δ_{ut}. For RANKL immature T cells are cleared at a rate δ_{ug} and immature T cells are also cleared more at a rate δ_u.

Equation (6) describes how uninfected mature T cells are produced at fixed rate δ_{ut} by the pool of immature T cells. These cells interact with any strain of the virus, V_k and become infected at rate $\beta_k = \beta\ \forall k$. The infectiousness parameter, β, is not constant over time, but depends on the interplay between viruses. In addition, T -cells are cleared out at fixed rate α_{ti}.

Equation (7) describes the infection of mature CD4+ T cells. Infected cells of strain k arise upon the interaction of a virus of strain k with any of the mature T cell strains. The infected cells, in turn, are cleared out at rate δ_i. In addition, the infected cells are added for cell to cell spreading of viruses at fixed rate α_{ti}.

Equation (8) describes the production of viral strains from infected cells at fixed rate π, viruses are cleared out at fixed rate δ_v.

Equation (9) describes the production of RANKL for HIV at fixed rate σ.

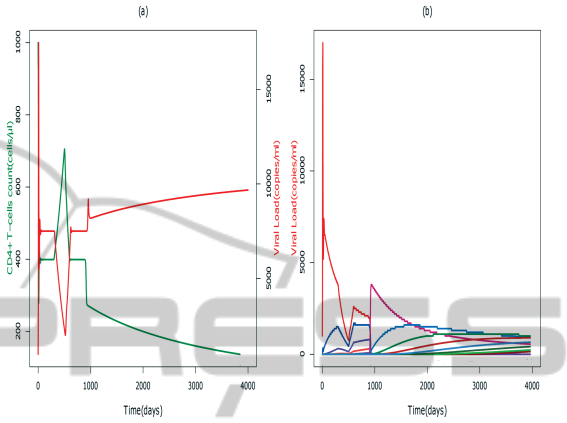

Figure 5: Therapy implemented from 200 days to 400 days a) CD4 +T cells count -green color (cells/ml) and corresponding viral load -red color (copies/ml) b) Effect on individual strain based viral load (copies/ml).

By using this model, it is possible to predict some scenarios of HAART treatment. HAART is one of the ways suppressing viral replication in the blood while attempting to prevent the virus rapidly developing resistance to the individual drug. The effect of the HAART treatment is simulated by an interval of time from 200 days to 400 days is reported in Figure. 5. Our results suggest that the drug treatment is able to increase the concentration of healthy CD4+ T-cells and decrease the concentration of virus and infected cells in the blood. So, with implementing the HAART therapy also changes the expression levels of RANKL, that effects on the bone remodelling. However, it is observed that after discontinuing the treatment, viral load increases again and hence concentration of CD4+ T-cells decreases. Moreover, we observed that short HAART treatments have small effect if administrated when CD4 +T cells count is above 200 and they have even smaller effect when CD4+ T cells counts are below 200.

4 CONCLUSIONS

From the meta analysis of gene expression data, we observe that like *S. aureus*, HIV-1 increases the osteomyelitis that impact on bone remodeling. HIV-1 virus upregulated and down regulated expression

level of some genes in the similar pattern of *S. aureus*. It is notable that the most important gene, RANKL, is down regulated in the both *S. aureus* and HIV infections. So we developed models for the bone remodeling including the effect of *S. aureus* caused osteomyelitis and HIV progression incorporating the effect of the RANKL that helps to gain better insight of the complexity of the disease progression. According to our model, HAART therapy can substantially decrease viral load and significantly increase CD4+ T cells, but it cannot eradicated virus completely even after implementing the therapy for a long time. From a methodological point of view this modelling approach has led to the proposal of considering additional estimators of the bone pathologies as diagnostic tool. That could also inspire the ideal situation in which a personalised model is generated from (personalised) data and the comparison between clinical data obtained during periodic medical check-up is compared with the computer predictions. Therefore our work is meaningful in perspective of a clinical bioinformatics characterized by a close coupling between clinical measures and modeling prediction.

REFERENCES

Ardura, M., Banchereau, R., Mejias, A., Di Pucchio, T., Glaser, C., Allantaz, F., Pascual, V., Banchereau, J., Chaussabel, D., and Ramilo, O. (2009). Enhanced monocyte response and decreased central memory t cells in children with invasive staphylococcus aureus infections. *PLoS One*, 4(5):e5446.

Claro, T., Widaa, A., O'Seaghdha, M., Miajlovic, H., Foster, T., O'Brien, F., and Kerrigan, S. (2011). Staphylococcus aureus protein a binds to osteoblasts and triggers signals that weaken bone in osteomyelitis. *PloS one*, 6(4):e18748.

Cummins, N., Klicpera, A., Sainski, A., Bren, G., Khosla, S., Westendorf, J., and Badley, A. (2011). Human immunodeficiency virus envelope protein gp120 induces proliferation but not apoptosis in osteoblasts at physiologic concentrations. *PloS one*, 6(9):e24876.

Gentleman, R., Carey, V., Bates, D., Bolstad, B., Dettling, M., Dudoit, S., Ellis, B., Gautier, L., Ge, Y., Gentry, J., et al. (2004). Bioconductor: open software development for computational biology and bioinformatics. *Genome biology*, 5(10):R80.

Gibellini, D., De Crignis, E., Ponti, C., Cimatti, L., Borderi, M., Tschon, M., Giardino, R., and Re, M. (2008). Hiv-1 triggers apoptosis in primary osteoblasts and hobit cells through tnfα activation. *Journal of medical virology*, 80(9):1507–1514.

Joshi-Tope, G., Gillespie, M., Vastrik, I., D'Eustachio, P., Schmidt, E., de Bono, B., Jassal, B., Gopinath, G., Wu, G., Matthews, L., et al. (2005). Reactome: a knowledgebase of biological pathways. *Nucleic acids research*, 33(suppl 1):D428–D432.

Komarova, S., Smith, R., Dixon, S., Sims, S., and Wahl, L. (2003). Mathematical model predicts a critical role for osteoclast autocrine regulation in the control of bone remodeling. *Bone*, 33(2):206–215.

Morabito, N. e. a. (2004). Osteoprotegerin and RANKL in the Pathogenesis of Thalassemia-Induced Osteoporosis: New Pieces of the Puzzle. *Journal of Bone and Mineral Research*, 19(5):722–727.

Parfitt, A. (1994). Osteonal and hemi-osteonal remodeling: The spatial and temporal framework for signal traffic in adult human bone. *Journal of cellular biochemistry*, 55(3):273–286.

Raggatt, L. and Partridge, N. (2010). Cellular and molecular mechanisms of bone remodeling. *Journal of Biological Chemistry*, 285(33):25103.

Ramilo, O., Allman, W., Chung, W., Mejias, A., Ardura, M., Glaser, C., Wittkowski, K., Piqueras, B., Banchereau, J., Palucka, A., et al. (2007). Gene expression patterns in blood leukocytes discriminate patients with acute infections. *Blood*, 109(5):2066–2077.

Reem, A., Manisha, H., Gary, D., Riana, C., Sohrab, D., Nora, G., Natasha, I., Nicole, M., Linda, P., Amy, G., et al. (2011). Osteoimmunopathology in hiv/aids: A translational evidence-based perspective. *Pathology research international*, 2011.

Sguanci, L., Bagnoli, F., and Lio, P. (2007). Modeling hiv quasispecies evolutionary dynamics. *BMC Evolutionary Biology*, 7(Suppl 2):S5.

Smoot, M., Ono, K., Ruscheinski, J., Wang, P., and Ideker, T. (2011). Cytoscape 2.8: new features for data integration and network visualization. *Bioinformatics*, 27(3):431–432.

Soetaert, K., Petzoldt, T., et al. (2010). Inverse modelling, sensitivity and monte carlo analysis in r using package fme. *Journal of Statistical Software*, 33(3):1–28.